AD-A094 989 AERONAUTICAL RESEARCH LABS MELBOURNE (AUSTRALIA) F/G 1/3
AN EXPERIMENTAL INVESTIGATION OF THE EFFECTS OF TRAILING-EDGE S--ETC(U)
MAR 80 G LONG, P A FARRELL
UNCLASSIFIED ARL/STRUC/NOTE-459 NL

1 OF 1
AD-
A094989

END
DATE
FILMED
3-81
DTIC

ARL-STRUC-NOTE-459 AR-001-808

(12)

DEPARTMENT OF DEFENCE

DEFENCE SCIENCE AND TECHNOLOGY ORGANISATION

AERONAUTICAL RESEARCH LABORATORIES

MELBOURNE, VICTORIA

STRUCTURES NOTE 459

AN EXPERIMENTAL INVESTIGATION OF THE EFFECTS OF TRAILING-EDGE STRIPS ON THE UNSTEADY AERODYNAMIC FORCES ON TABS

by

G. LONG and P. A. FARRELL

Approved for Public Release.

COPY No 15

MARCH 1980

81 2 13 022

AR-001-808

DEPARTMENT OF DEFENCE
DEFENCE SCIENCE AND TECHNOLOGY ORGANISATION
AERONAUTICAL RESEARCH LABORATORIES

STRUCTURES NOTE-459

AN EXPERIMENTAL INVESTIGATION OF THE EFFECTS OF TRAILING-EDGE STRIPS ON THE UNSTEADY AERODYNAMIC FORCES ON TABS

by

G. LONG and P. A. FARRELL

SUMMARY

An investigation into the effect on unsteady aerodynamic forces of attaching trailing-edge strips to a control surface is described. Results from a brief series of two-dimensional wind-tunnel tests are compared with classical thin lifting surface calculations.

POSTAL ADDRESS: Chief Superintendent, Aeronautical Research Laboratories,
Box 4331, P.O., Melbourne, Victoria, 3001, Australia.

DOCUMENT CONTROL DATA SHEET

Security classification of this page: Unclassified

1. Document Numbers (a) AR Number: AR-001-808 (b) Document Series and Number: Structures Note 459 (c) Report Number: ARL-Struc-Note-459	2. Security Classification (a) Complete document: Unclassified (b) Title in isolation: Unclassified (c) Summary in isolation: Unclassified

3. Title: AN EXPERIMENTAL INVESTIGATION OF THE EFFECTS OF TRAILING-EDGE STRIPS ON UNSTEADY AERODYNAMIC FORCES ON TABS

4. Personal Author(s): G. Long P. A. Farrell	5. Document Date: March, 1980 6. Type of Report and Period Covered:
7. Corporate Author(s): Aeronautical Research Laboratories 9. Cost Code: 23 5000	8. Reference Numbers (a) Task: PDY 78/02 (b) Sponsoring Agency:
10. Imprint Aeronautical Research Laboratories, Melbourne.	11. Computer Program(s) (Title(s) and language(s)):

12. Release Limitations (of the document)
Approved for public release.

12-0. Overseas:	N.O.		P.R.	1	A		B		C		D		E	

13. Announcement Limitations (of the information on this page):
No limitation.

14. Descriptors:		15. Cosati Codes:
Control surfaces	Flutter	0103
Boundary layer control	Spoilers	2004
Unsteady flow		

16. *ABSTRACT*

An investigation into the effect on unsteady aerodynamic forces of attaching trailing-edge strips to a control surface is described. Results from a brief series of two-dimensional wind-tunnel tests are compared with classical thin lifting surface calculations.

CONTENTS

NOTATION

L	$\frac{1}{2}\rho v^2 l (Q_1' + i\nu Q_1'')be^{i\omega t}$
M	$\frac{1}{2}\rho v^2 l^2 (Q_2' + i\nu Q_2'')be^{i\omega t}$
HM	$\frac{1}{2}\rho v^2 l^2 (Q_3' + i\nu Q_3'')be^{i\omega t}$
L	aerodynamic force on wing, positive upwards
M	aerodynamic moment about wing leading edge, positive nose down
HM	aerodynamic moment about control hinge line, positive nose down
ρ	air density
v	velocity of air
l	chord of wing
ν	frequency parameter $\omega l/v$
ω	circular frequency of vibration
t	time
b	amplitude of control rotation, radians, positive tail down
Q_1' Q_2' Q_3'	real parts of generalised forces
Q_1'' Q_2'' Q_3''	imaginary parts of generalised forces
$\frac{1}{2}\rho v^2$	factor used to non-dimensionalise measured pressures.

1. INTRODUCTION

A fairly common problem on new aircraft is that of achieving good control surface effectiveness. Often boundary layer thickness and interference from other surfaces may cause flow separation on all or part of the control. This reduces control efficiency and can cause serious problems in achieving good control of aircraft response. These types of problems are difficult to predict analytically or from wind-tunnel tests. Usually the first evidence of such difficulties occurs during prototype flying and consequently serious efforts must be made to find a 'fix' which can be introduced fairly simply and cheaply at a late stage in the design. These 'fixes' often involve vortex generators, placed on or ahead of the control, or thickening of the trailing edge of the control. The latter may be simply achieved by attaching a small angle to one or both sides of the control along the trailing edge ~~(see Fig. 1).~~ The aim of these and other methods is to improve the effectiveness of the control and hopefully to increase this to its theoretical or design value.

While the effect of such modifications is fairly well known for steady flow, little evidence is available of the effect in unsteady flow. There are no theoretical methods of predicting unsteady aerodynamic forces on oscillating control surfaces which have vortex generators or trailing-edge angles attached as in Figure 1. Usually complete reliance is based on classical thin lifting surface theories for predicting flutter speeds and frequencies. In Reference 1 the user of such control surface 'fixes' is cautioned that they may have a very powerful effect on flutter properties. In Reference 2 details are given of a flutter incident involving a similar type of trailing-edge thickening device.

The work described was undertaken as a result of an accident to the Nomad aircraft ~~(Ref. 3)~~ in which flutter occurred as a result of fitting trailing-edge strips to the tailplane tabs. This flutter occurred at an unusually high value of frequency parameter (4·5 based on tailplane chord), and it was considered worthwhile to undertake an experimental investigation to determine the unsteady aerodynamic forces on the configuration used.

The results presented were obtained in a fairly short period of wind tunnel testing and were not as comprehensive as would normally be desired; however it is considered that the data should be of interest to flutter engineers as they provide an insight into the effects of trailing-edge strips on unsteady aerodynamic derivatives.

2. DESCRIPTION OF TESTS

2.1 Wind-tunnel Model

No attempt was made to construct a scale model of the tailplane. Instead a section of the full-scale tailplane was instrumented and mounted between large end plates 1·52 m apart in the ARL 9 × 7 wind-tunnel thus forming a two-dimensional test section (see Fig. 2). The tailplane, which is of symmetrical section (NACA 0015), was clamped rigidly by the end walls. The tab, which was attached with a standard piano-hinge, was rotated by means of push rods fitted at each end.

Pressure tappings were made on the section on both top and bottom surfaces at the locations given in Table 1. A drawing of the method of installing each tube is given in Figure 3. Each pressure tapping was connected by a 1·2 mm inside diameter tube to a 24 port acoustical scanning valve. This valve was used because its internal construction was such as to avoid all discontinuities or sharp corners. The valve was connected to a long length of tubing so that the single pressure transducer measured the pressure at one point of a pressure tube, which was effectively infinitely long (see Figure 4). In this way problems due to tube resonances were avoided. Each tube was individually calibrated at each frequency of oscillation by applying a known sinusoidal pressure at the inlet and comparing this with the outlet pressure. At the low velocities of the tests, errors due to the mean air flow velocity past the end of the tube are small (see Ref. 4).

The tab was oscillated by two electromagnetic shakers mounted outside the tunnel and connected by push rods to each end of the tab. Tab motion was monitored by an accelerometer and a velocity transducer at each end.

All the transducer signals were measured by means of a digital transfer function analyser which averaged the reading over 100 cycles of oscillation in order to reduce the effect of noise.

The major dimensions of the model are given in Table 3.

2.2 Test Procedure

The wind-tunnel speed was maintained constant at either 41·2 m/sec or 51·5 m/sec and the tab oscillated through approximately $\pm 1°$. Four excitation frequencies were used: -5 Hz, 10 Hz, 20 Hz and 30 Hz. This resulted in a range of frequency parameters (based on model chord) of approximately 0·7 to 5·7.

Initial tests were conducted on the model without trailing-edge strips, then tests were performed with either 2·54 cm or 5·08 cm strips fitted. The effect of a mean tab deflection of approximately 1·27° was also investigated.

At each tunnel speed the tab was oscillated at constant amplitude and frequency, whilst the pressures were read individually by stepping the scanning valve from port to port. Only 24 surface pressures were measured in any one test.

The tab used on the model was a standard aircraft tab and the only modifications made to it were to provide transducer and pushrod mountings and to install pressure tappings. During oscillation the amplitudes of oscillation of each end of the tab were maintained equal and in-phase; however, some bending of the tab occurred which resulted in the centre of the tab having a greater amplitude than the ends. This effect varied with frequency as shown in Figure 5. Little difference in vibration mode shape occurred between the tests when the trailing-edge strips were on or off, the main effect being a gradual increase in the amount of tab bending with increase in frequency. Since the pressures were measured along the centre-line of the model it was considered desirable to use the centre-line amplitude of the tab as the controlling parameter when normalising the measured pressures. The appropriate scale factors, defining the ratio of centre-line amplitude to the mean amplitude of the ends, are given in Table 2.

3. RESULTS AND DISCUSSION

3.1 General

The pressures obtained were corrected for wind-tunnel blockage and non-dimensionalised with respect to the free-stream dynamic pressure. These pressure coefficients are plotted as modulus and phase angle against chordwise position. Both upper and lower surface pressures are plotted on each figure. In the phase angle graphs the phase angles of the upper surface pressures are changed π radians so that they can be directly compared with the lower surface values.

3.2 No T-strips Fitted

The pressure distributions, obtained when no T-strips were attached to the tab, are presented in Figures 6 and 7. Also shown in these figures are the theoretical values obtained using the method of Reference 5. In this method Possio's integral equation for two-dimensional unsteady flow has been solved using the doublet lattice technique. A total of 100 equal chord strips was used to calculate the pressures for each value of frequency.

In general the modulus of pressure, determined experimentally, is everywhere less than the theoretical value. The agreement between experimental and theoretical phase angles is good on the main surface but poor near the trailing-edge of the tab where the pressures are tending to zero. The experimental and theoretical data exhibit similar behaviour as frequency parameter is increased.

3.3 Tab with 2·54 cm T-strips

In Figures 8 and 9 the pressure distributions for the tab with T-strips are presented for three values of frequency parameter ν (written as NU in the figures). When these results are compared with those obtained without T-strips the most striking differences are the increased values of pressure obtained on the tab and the very large change in phase angle. Whereas in Figure 6 (no T-strips) the pressure at the trailing-edge falls to zero, in Figures 8 and 9 a finite pressure occurs. The phase response on the tab, which varies from approximately zero at the hinge to $\pi/2$ at the trailing-edge, when no strips are fitted, is approximately constant over the tab when strips are used. Over the fixed portion of the surface the modulus of the pressure increases slightly when T-strips are fitted and the phase angle decreases.

3.4 Tab with 5·08 cm T-strips

The pressure distributions, obtained for this configuration, are plotted in Figures 10 to 12 for the five values of frequency parameter used. These data are similar to those presented in Figures 8 and 9 for the 2·54 cm T-strips and indicate slight increases in the magnitude of the pressures but almost exactly the same phase response.

The net effect of the T-strips on the control surface derivatives, obtained by integrating the measured pressure distributions, is shown in Table 4A. In this table, the lift, moment about the leading edge and control hinge-moment are tabulated as modulus and phase angle and also as real and imaginary parts, for each value of frequency parameter.

3.5 Effect of Mean Tab Deflection

In order to determine the effect of a mean tab deflection on the oscillatory pressures the tab mean position was adjusted so that, at the operating speed, the tab mean incidence was 1·27 degrees. The results of these tests, for oscillations of the tab fitted with the 5·08 cm T-strips, are presented in Figures 13 and 14 for three values of frequency parameter. There are no significant differences in character between these results and those in Figures 10 to 12 for the control with no mean deflection, although there is evidence that the top and bottom surface pressures are no longer equal.

The forces and moments, obtained by integrating these pressures (see Table 4B), are compared with the data from the tests with no mean tab deflection in Figures 18 to 20. Inspection of these figures reveals that the major difference in the results is in the phase angle of response. In all instances the phase angles obtained with the control deflected are closer to the theoretical values than the no-deflection data.

3.6 Discussion

The theoretical and experimental pressure distributions for the tab without T-strips are compared in Figures 6 and 7. These show that the theory overestimates the pressures due to control rotation by approximately 50%. This is to be expected for a thick aerofoil and a small control surface, since the boundary layer is thickest in the region of the trailing-edge and this reduces the effectiveness of the control. The degree of agreement between the experimental and theoretical data compares favourably with results of other experiments (see Ref. 6).

In Figures 15 to 17 the data of Table 4A are plotted and compared with theoretical derivatives obtained from Reference 5. In Figure 14 the modulus and phase of the lift due to control rotation are shown. When no T-strips are fitted the measured lifts are approximately 70% of the theoretical values, whereas the measured phase angles are in closer agreement with the theory. When T-strips are fitted the magnitude of the lift increases to exceed the theoretical values for most frequency parameters investigated, but the phase angle decreases substantially. The forces generated by the larger T-strips are only slightly greater than those due to the small strips; however the change in phase angle is not significantly affected by T-strip size.

The moment about the leading edge due to control rotation is presented in Figure 16. Again the magnitudes of the experimental data are approximately 70% of the theoretical values, but there is much closer agreement between the phase angles. When T-strips are fitted the magnitude of the moment increases substantially and the phase angle decreases.

As in Figure 15 the differences between small and large T-strips are more pronounced on the magnitude of the moment than on the phase angle.

In Figure 17 the control surface hinge moments both theoretical and experimental, are compared. In this instance the effects of T-strips are more pronounced. The "no-strip" experimental data vary from 45% to 63% of the theoretical values and are as little as one sixth of the 5·08 cm T-strip data. Again the theoretical phase angles compare reasonably well with the no-T-strip experimental data, but differ significantly from the T-strip-fitted data. For the latter data the difference between theoretical and experimental phase angles increases with increase in size of the T-strips.

Only one value of mean tab deflection was investigated and the results of this test, presented in Figures 18 to 20, indicate that the major influence of tab deflection is on phase angle of response. There is however some indication in Figures 13 and 14 that the pressures on top and bottom surfaces, especially on the control, are no longer equal.

4. CONCLUSIONS

1. The addition of T-strips to a control surface significantly increases the pressures on the control and creates a step change in pressure at the trailing-edge. There is a significant increase in control hinge moment and a large change in the phase angle of response.

2. The lift and pitching moment about the leading edge, due to control rotation, are both increased by the addition of T-strips to the trailing edge; however the phase angle of response is decreased.

3. The larger T-strips in general, increased the magnitude of all the derivatives, more than the small strips.

4. A mean tab deflection of 1·27 degrees had a small effect on the derivatives, although it created a significant difference between the upper and lower surface pressures.

REFERENCES

1. Broadbent, E. G. The elementary theory of aero-elasticity. Aircraft Engineering March–June 1954.

2. Niblett, Ll. T. Flutter calculations on a rudder with trailing-edge spoiler. R.A.E. Report Structures 202, May 1956.

3. —— Report on investigation of tailplane flutter. GAF N24 Nomad Aircraft at Avalon, Victoria, on 6 August 1976. Dept. of Transport, Australia. Special Investigation Report 77-1.

4. Tijdeman, H. Investigations of the transonic flow around oscillating airfoils. NLR TR 77090U.

5. Farrell, P. A. A fortran program to calculate two-dimensional, subsonic oscillatory aerodynamic forces, based on doublet lines. ARL Memo to be published.

6. Tijdeman, H. and Bergh, H. Analysis of pressure distributions on a wing with oscillating control surface in two-dimensional high subsonic and transonic flow. NLR TR F253, 1969.

TABLE 1

Locations of Pressure Tubes on Model

Tube Positions
% Chord from Leading Edge

Upper Surface	Lower Surface
0·042	0·082
0·115	0·175
0·24	0·319
0·388	0·481
0·551	0·654
0·69	0·768
0·798	0·835
0·842	0·888
0·887	0·915
0·911	0·948
0·946	0·982
0·983	

TABLE 2

Amplitude Ratios Used to Normalise Test Data

Frequency	Amplitude Ratio
5 Hz	1·0
10 Hz	1·04
20 Hz	1·21
30 Hz	1·40

TABLE 3

Major Dimensions of Model

Chord	52 inches	1·32 m
Tab Chord	7 inches	0·178 m
Span	59·8 inches	1·52 m
Aerofoil Section	NACA 0015	

TABLE 4A

Summary of Experimental Derivatives
(No Control Deflection)

	$\nu \simeq 0\cdot75$		$\nu \simeq 1\cdot6$			$\nu \simeq 3\cdot1$			$\nu \simeq 4\cdot8$			$\nu \simeq 5\cdot7$	
	T-strips 5·08 cm	No Strips	T-strips 2·54 cm	T-strips 5·08 cm	No Strips	T-strips 2·54 cm	T-strips 5·08 cm.	No Strips	T-strips 2·54 cm	T-strips 5·08 cm	No Strips	T-strips 2·54 cm	T-strips 5·08 cm
Q_1'	2·030	1·072	1·922	2·164	1·082	1·706	1·958	1·216	1·771	2·114	1·370	—	2·086
Q_2'	1·091	0·580	1·150	1·270	0·608	1·066	1·215	0·688	1·124	1·318	0·753	—	1·262
Q_3'	0·033	0·006	0·034	0·041	0·006	0·030	0·038	0·006	0·028	0·038	0·006	—	0·032
Q_1''	−0·917	0·032	0·268	0·283	0·092	−0·024	−0·030	0·109	0·048	0·036	0·141	—	0·104
Q_2''	−0·200	0·063	0·018	0·026	0·092	0·036	0·042	0·102	0·066	0·062	0·118	—	0·106
Q_3''	0·002	0·003	0·002	0·003	0·003	0·002	0·002	0·004	0·002	0·002	0·004	—	0·003
Q_1	2·138	1·074	1·970	2·208	1·118	1·708	1·960	1·326	1·786	2·122	1·606	—	2·174
Q_2	1·101	0·588	1·150	1·270	0·672	1·072	1·222	0·844	1·168	1·352	1·024	—	1·408
Q_3	0·033	0·008	0·034	0·042	0·012	0·030	0·038	0·018	0·030	0·040	0·024	—	0·036
$\angle Q_1$	0·318	0·048	−0·220	−0·200	0·258	−0·044	−0·044	0·410	0·129	0·082	0·549	—	0·286
$\angle Q_2$	−0·133	0·175	−0·025	−0·033	0·439	0·104	0·107	0·618	0·275	0·222	0·747	—	0·460
$\angle Q_3$	−0·042	0·675	0·131	0·073	1·025	0·204	0·162	1·216	0·419	0·247	1·318	—	0·505

TABLE 4B

Summary of Experimental Derivatives

(Control Deflected)

	$\nu \simeq 1{\cdot}6$	$\nu \simeq 3{\cdot}1$	$\nu \simeq 4{\cdot}6$
Q_1'	1·984	1·888	2·120
Q_2'	1·218	1·180	1·344
Q_3'	0·032	0·032	0·032
Q_1''	−0·234	0·018	0·090
Q_2''	0·034	0·086	0·102
Q_3''	0·046	0·004	0·004
$\lvert Q_1\rvert$	2·016	1·890	2·160
$\lvert Q_2\rvert$	1·220	1·209	1·424
$\lvert Q_3\rvert$	0·037	0·034	0·038
$\angle Q_1$	−0·178	0·031	0·193
$\angle Q_2$	0·044	0·221	0·339
$\angle Q_3$	0·220	0·363	0·537

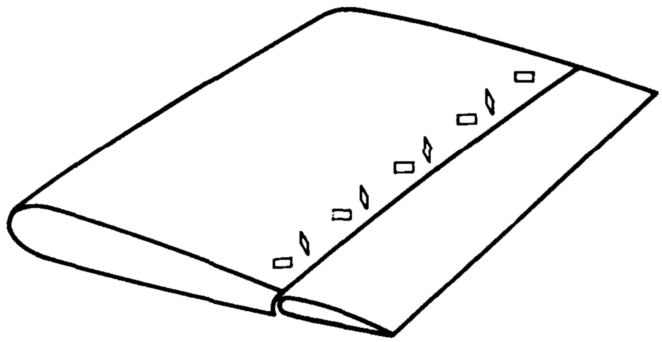

Vortex generators at leading edge of control

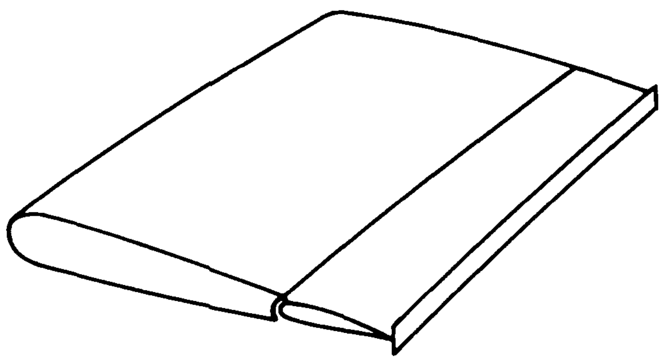

T-strips at trailing edge of control

FIG. 1: EXAMPLES OF TECHNIQUES USED TO IMPROVE CONTROL EFFECTIVENESS

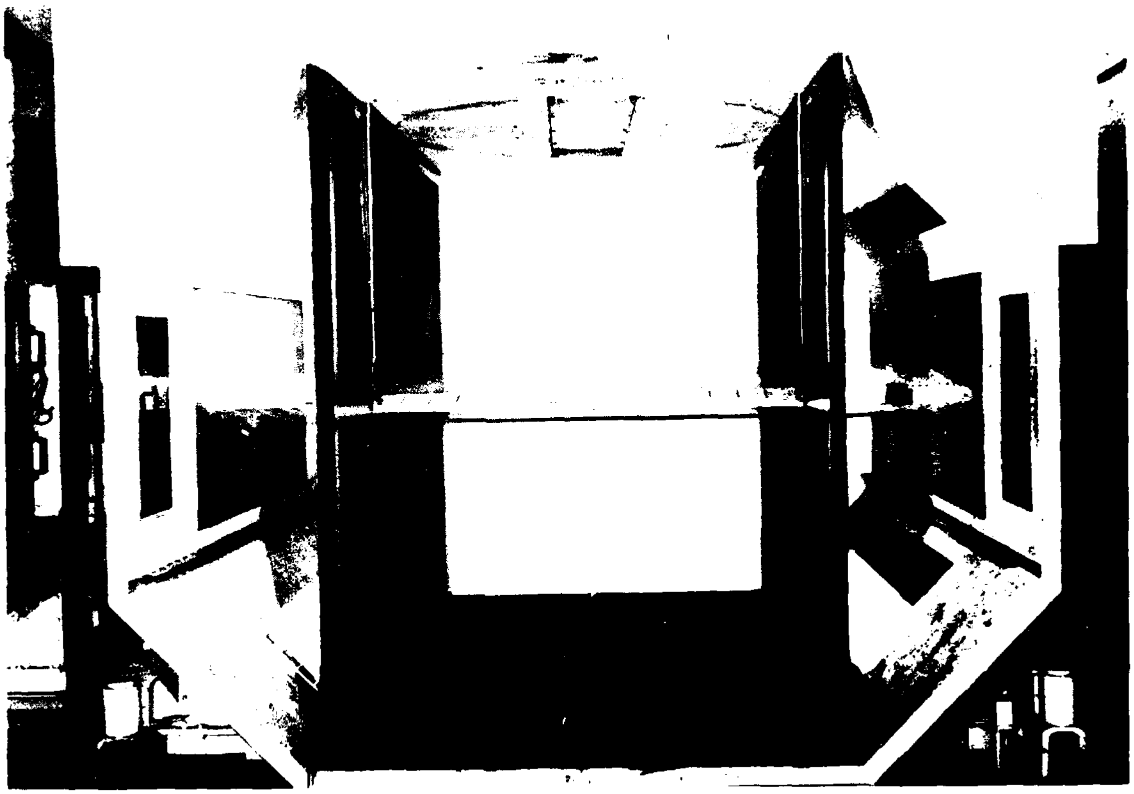

FIG. 2: WIND TUNNEL MODEL MOUNTED IN WORKING SECTION OF TUNNEL

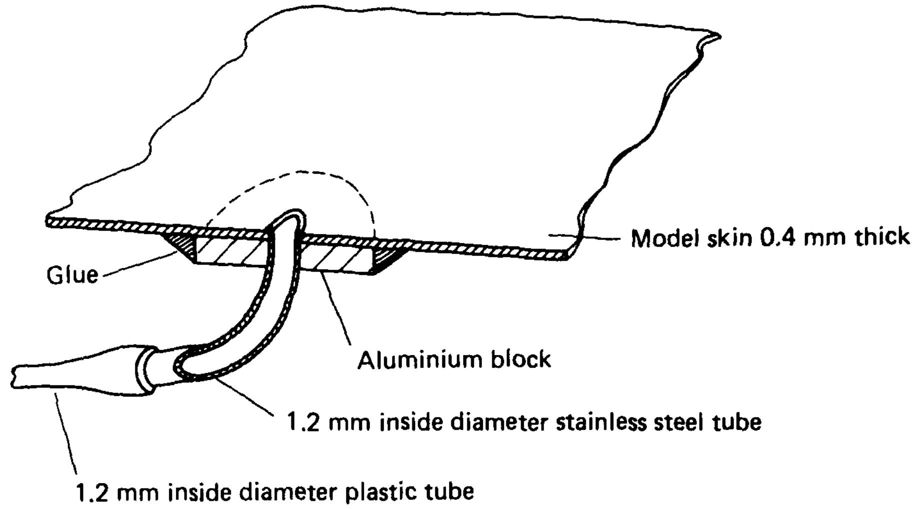

FIG. 3: METHOD OF INSTALLING PRESSURE TAPPING IN MODEL SKIN

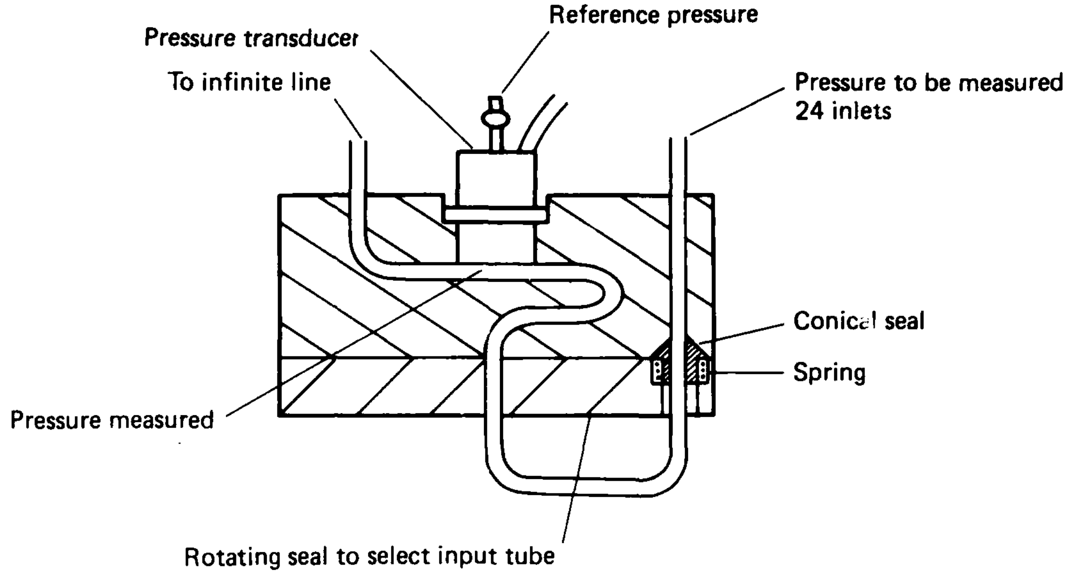

FIG. 4: DETAIL OF SCANI-VALVE SYSTEM

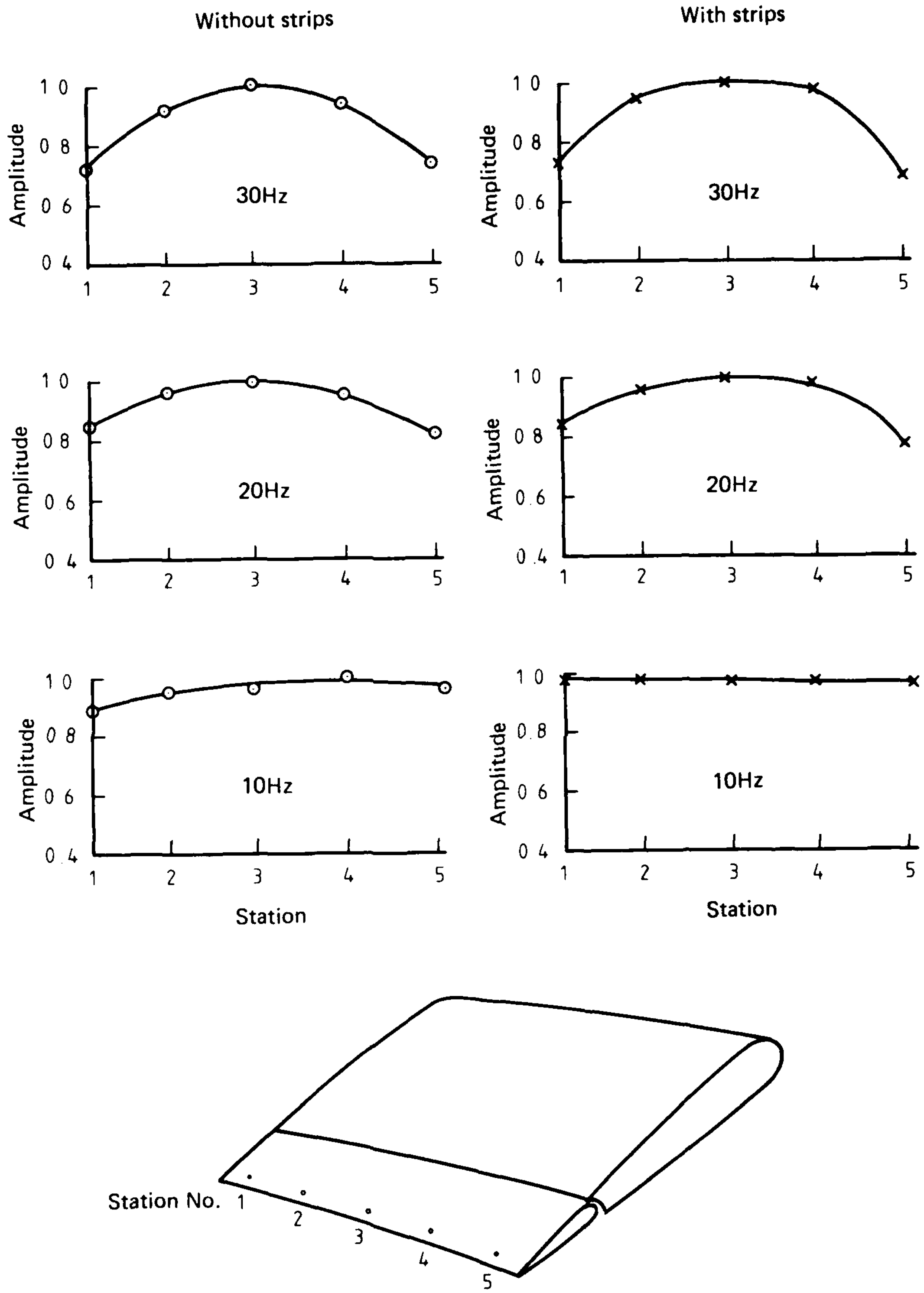

FIG. 5: VIBRATION MODE SHAPES OF TABS AT 10, 20, 30Hz

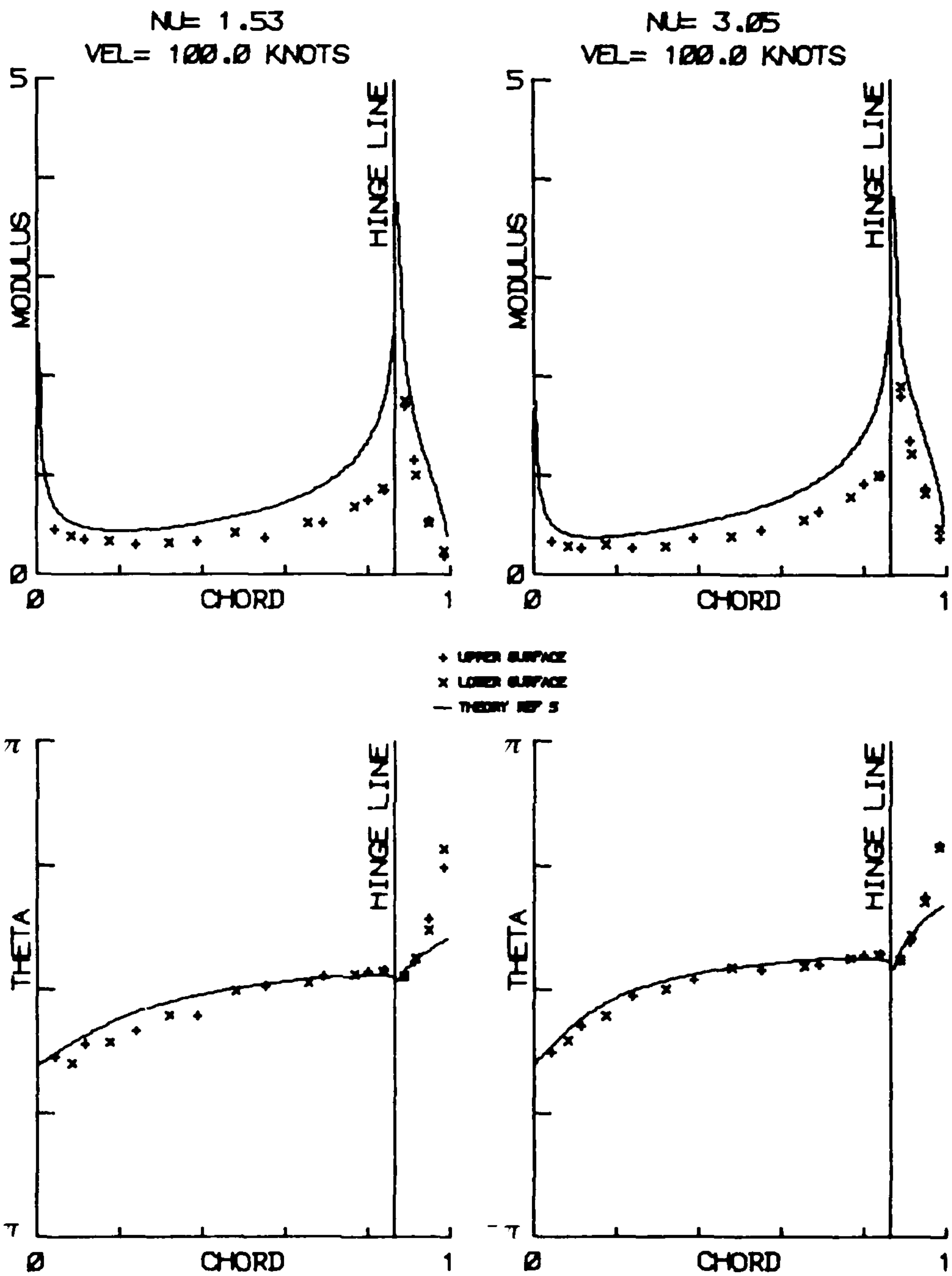

FIG. 6: CHORDWISE VARIATION OF PRESSURE (MODULUS AND PHASE ANGLE) NO CONTROL DEFLECTION NO T-STRIPS

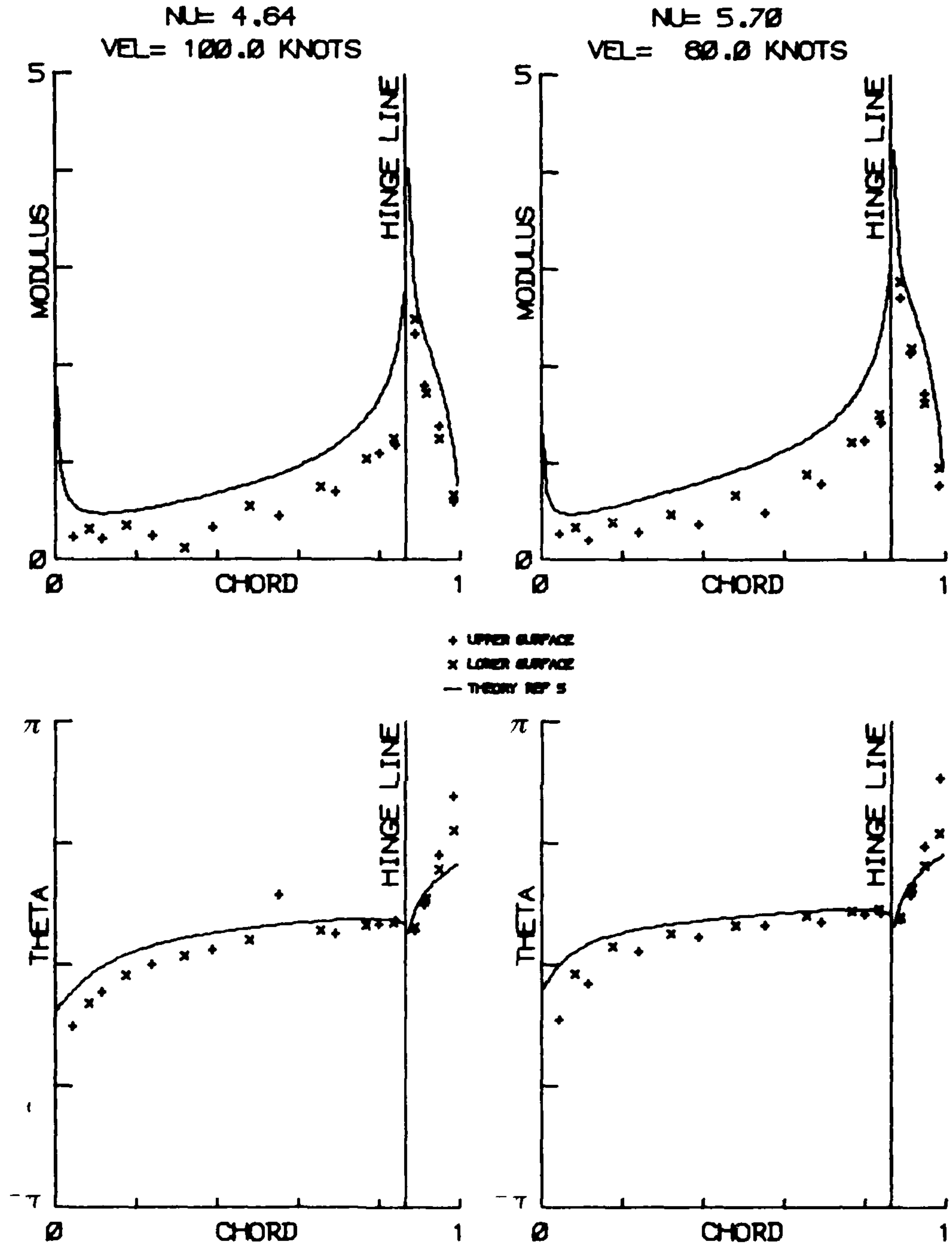

FIG. 7: CHORDWISE VARIATION OF PRESSURE (MODULUS AND PHASE ANGLE)
NO CONTROL DEFLECTION NO T-STRIPS

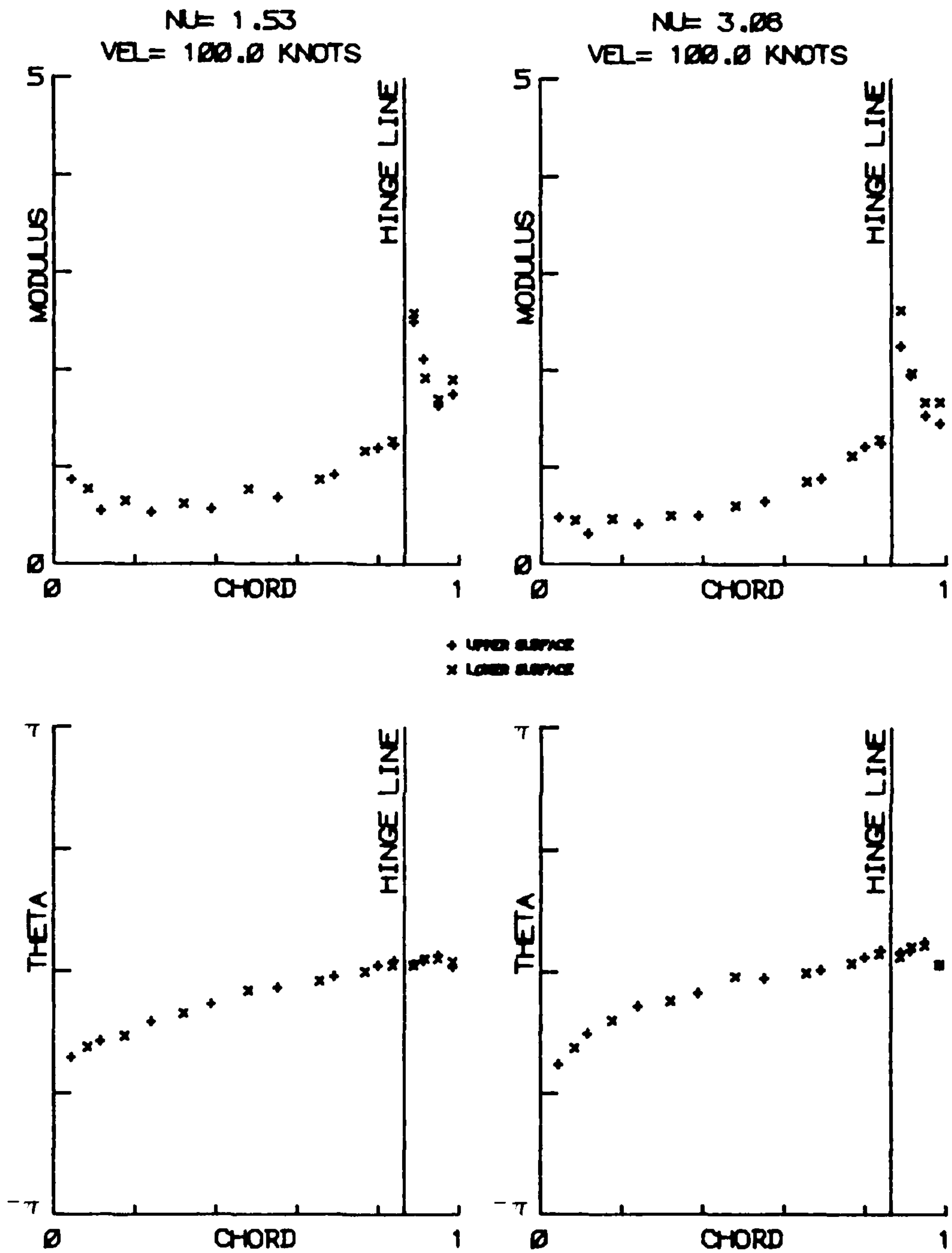

FIG. 8: CHORDWISE VARIATION OF PRESSURE (MODULUS AND PHASE ANGLE)
NO CONTROL DEFLECTION 2.54CM T-STRIPS

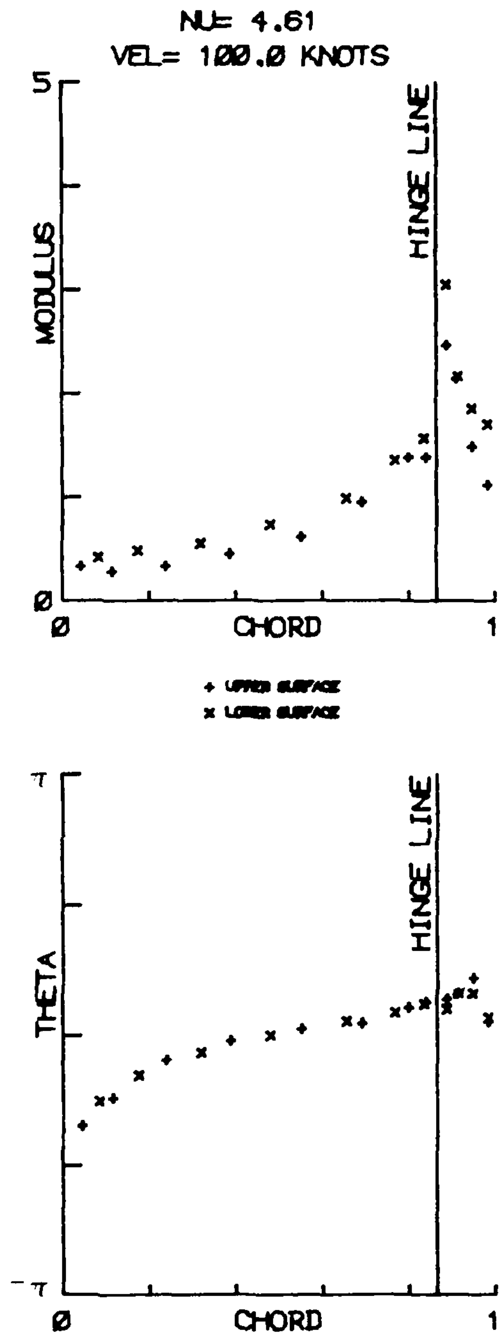

FIG. 9: CHORDWISE VARIATION OF PRESSURE (MODULUS AND PHASE ANGLE)
NO CONTROL DEFLECTION 2.54CM T-STRIPS

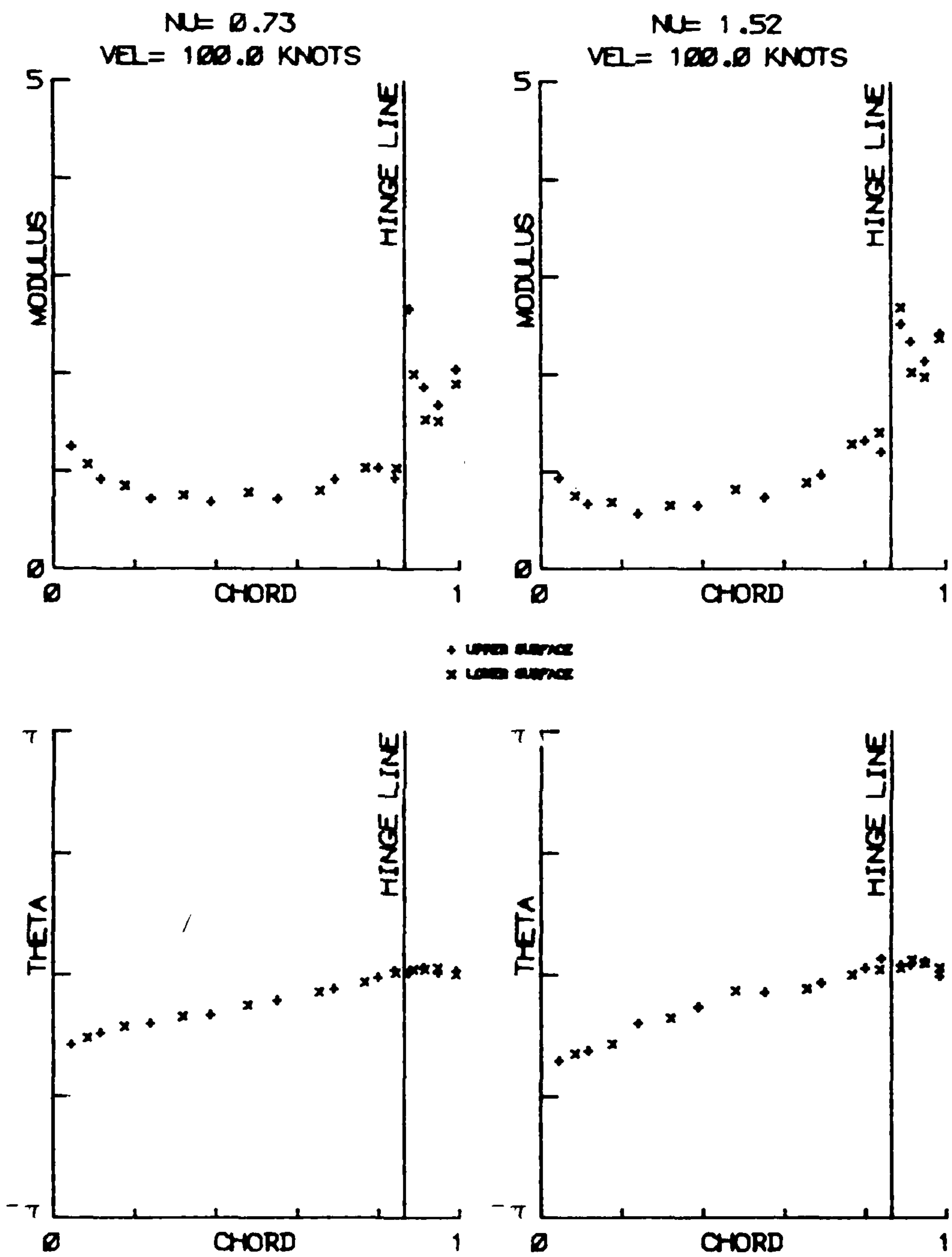

FIG. 10: CHORDWISE VARIATION OF PRESSURE (MODULUS AND PHASE ANGLE)
NO CONTROL DEFLECTION 5.08CM T-STRIPS

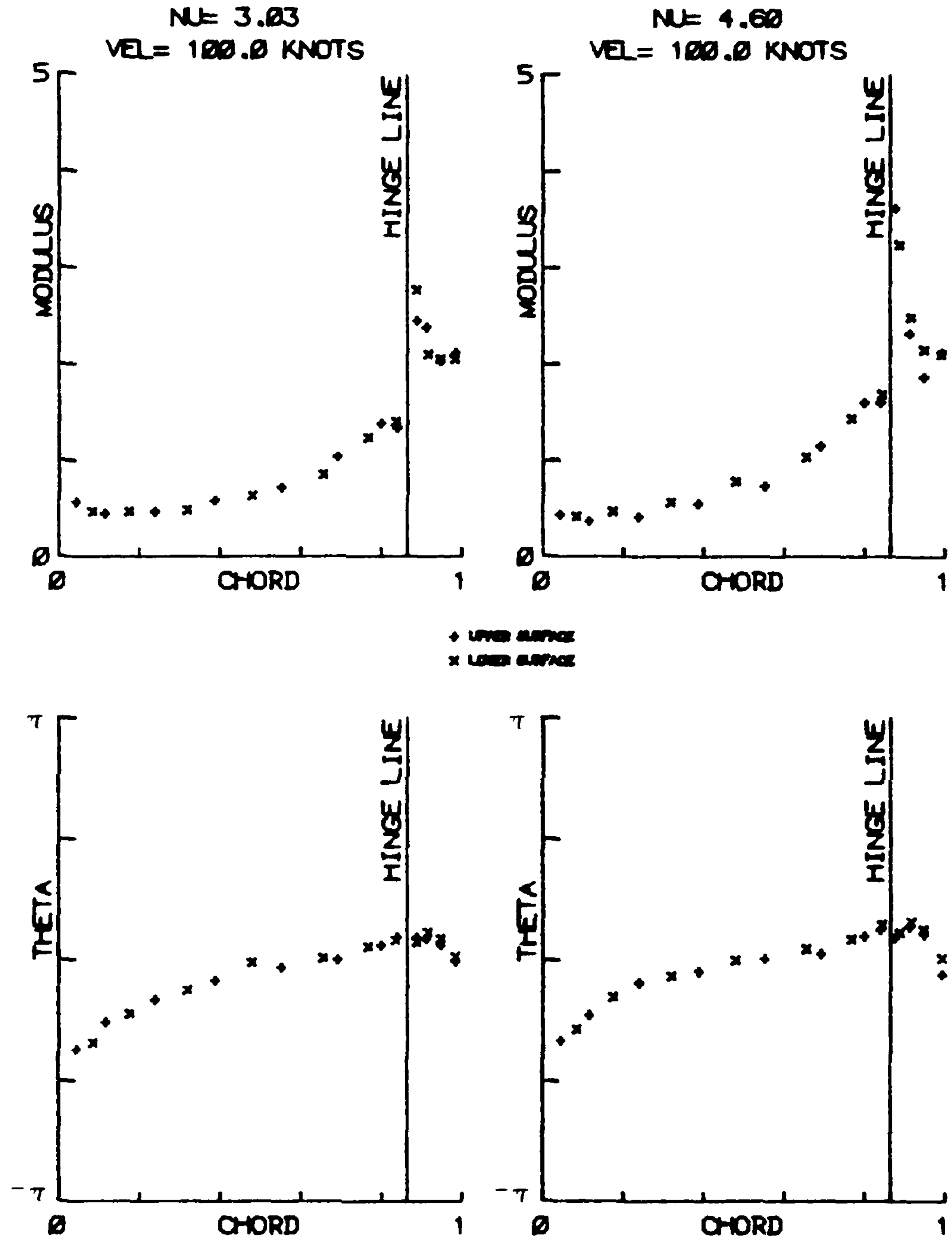

FIG. 11: CHORDWISE VARIATION OF PRESSURE (MODULUS AND PHASE ANGLE)
NO CONTROL DEFLECTION 5.08CM T-STRIPS

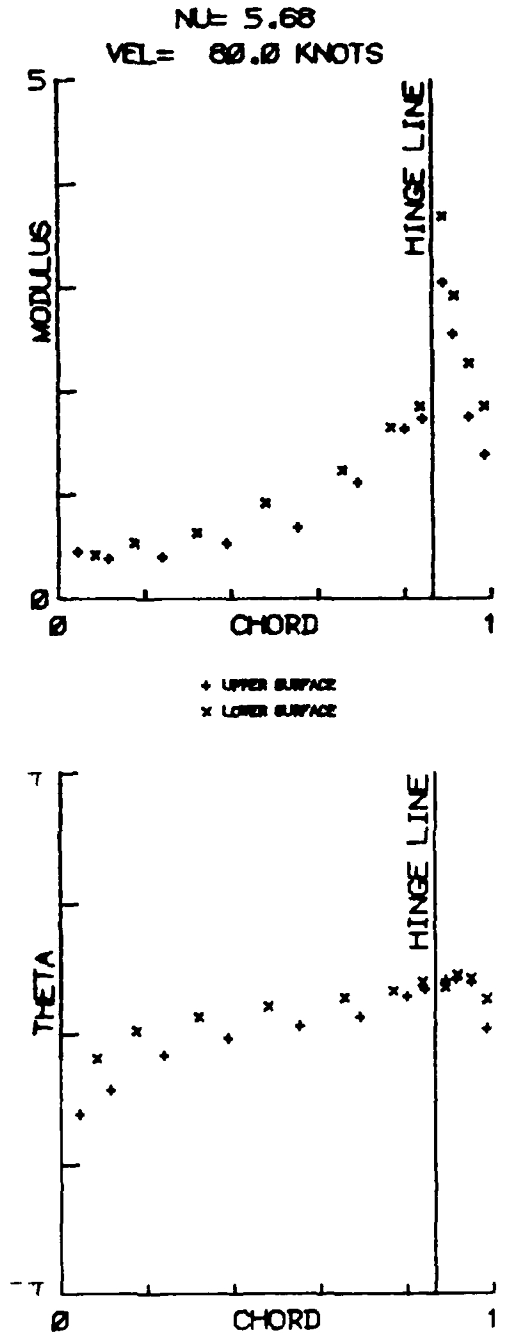

FIG. 12: CHORDWISE VARIATION OF PRESSURE (MODULUS AND PHASE ANGLE)
NO CONTROL DEFLECTION 5.08CM T-STRIPS

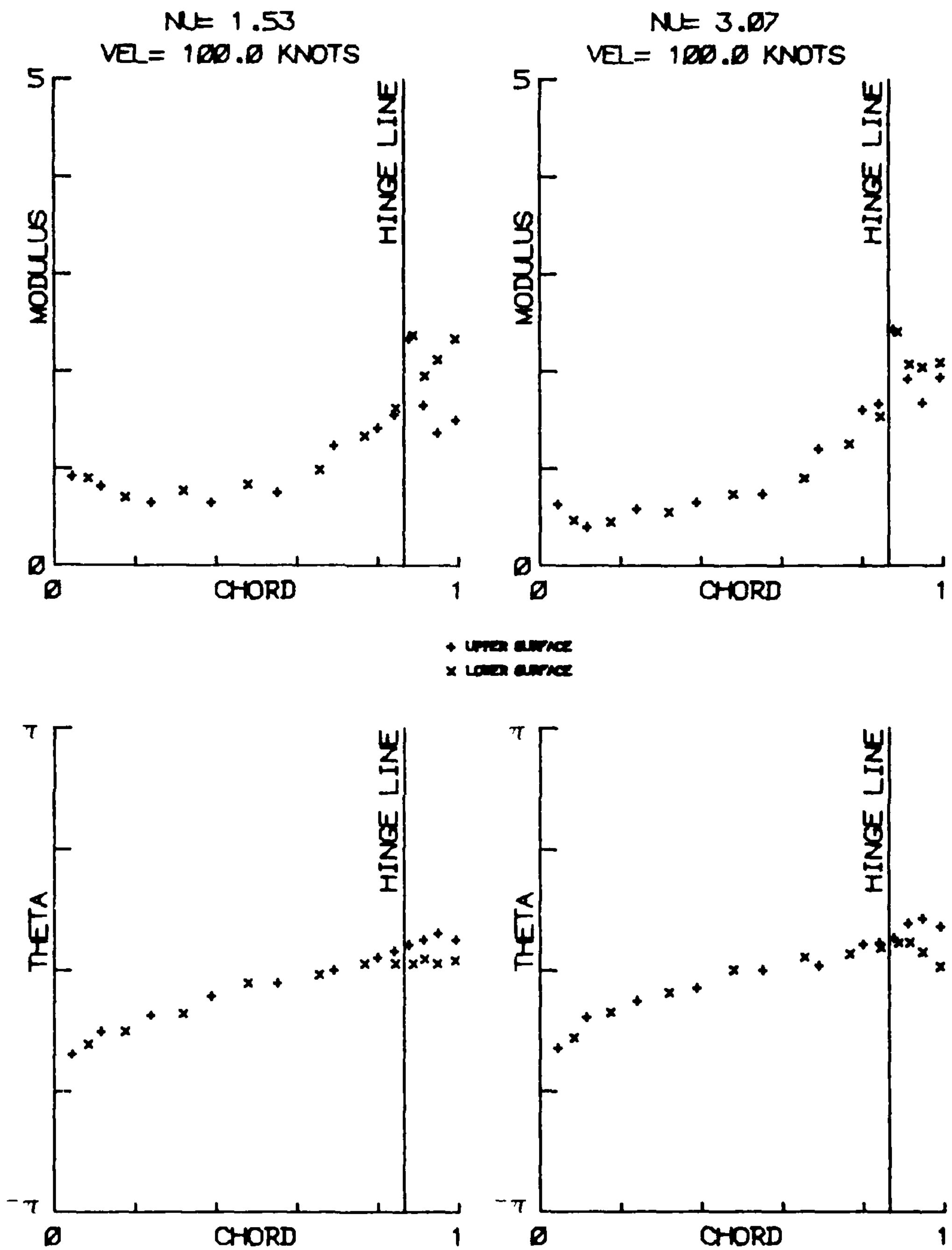

FIG. 13: CHORDWISE VARIATION OF PRESSURE (MODULUS AND PHASE ANGLE) CONTROL DEFLECTED 5.08CM T-STRIPS

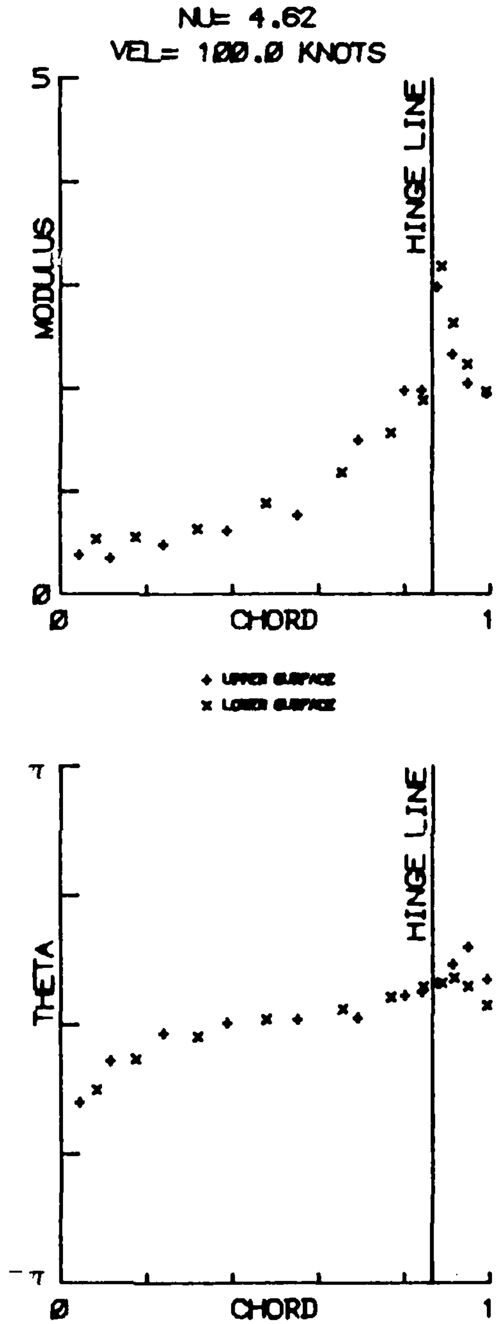

FIG. 14: CHORDWISE VARIATION OF PRESSURE (MODULUS AND PHASE ANGLE)
CONTROL DEFLECTED 5.08CM T-STRIPS

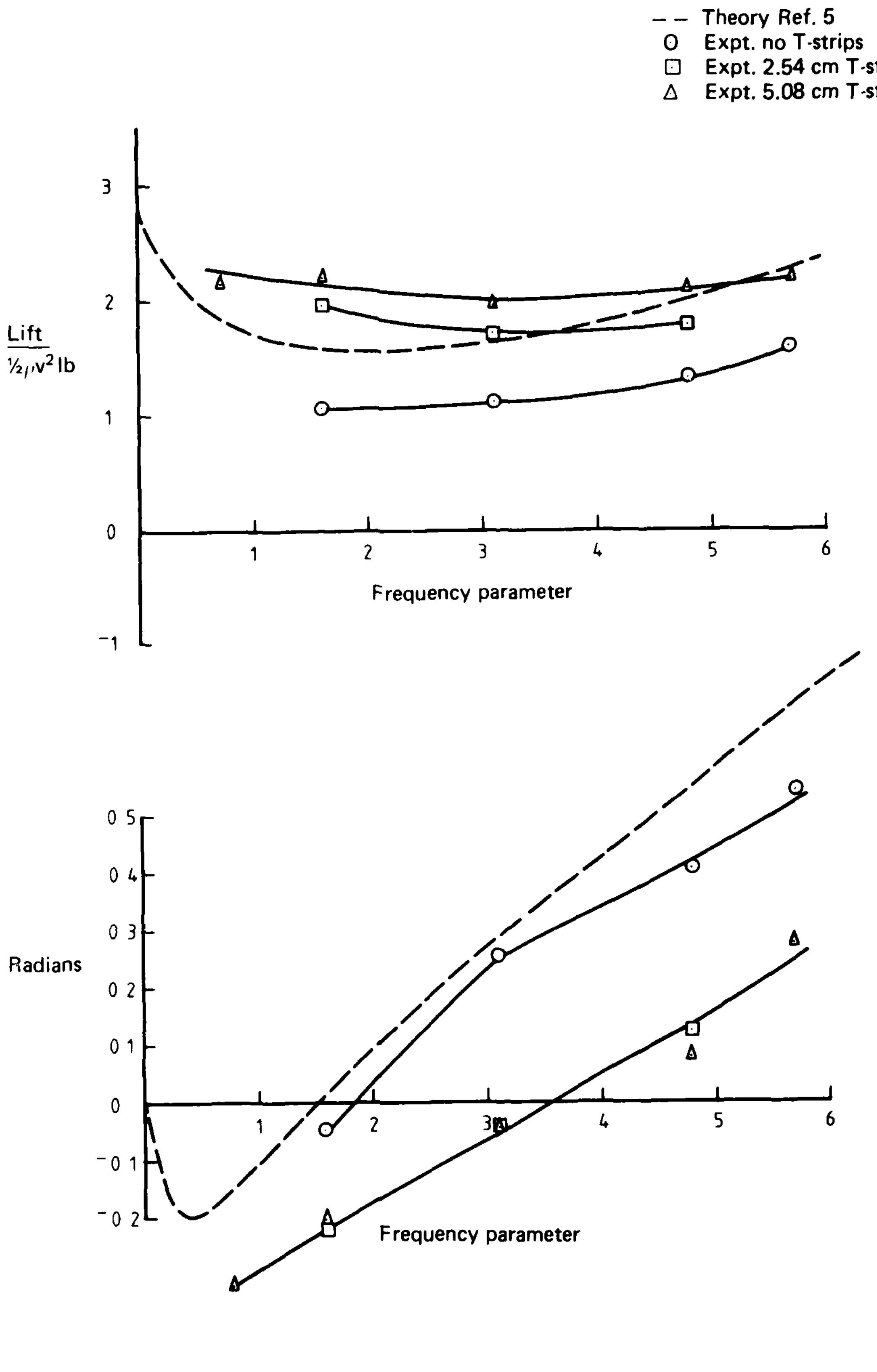

FIG. 15: COMPARISON OF THEORETICAL AND EXPERIMENTAL DERIVATIVES
(Lift due to control rotation)

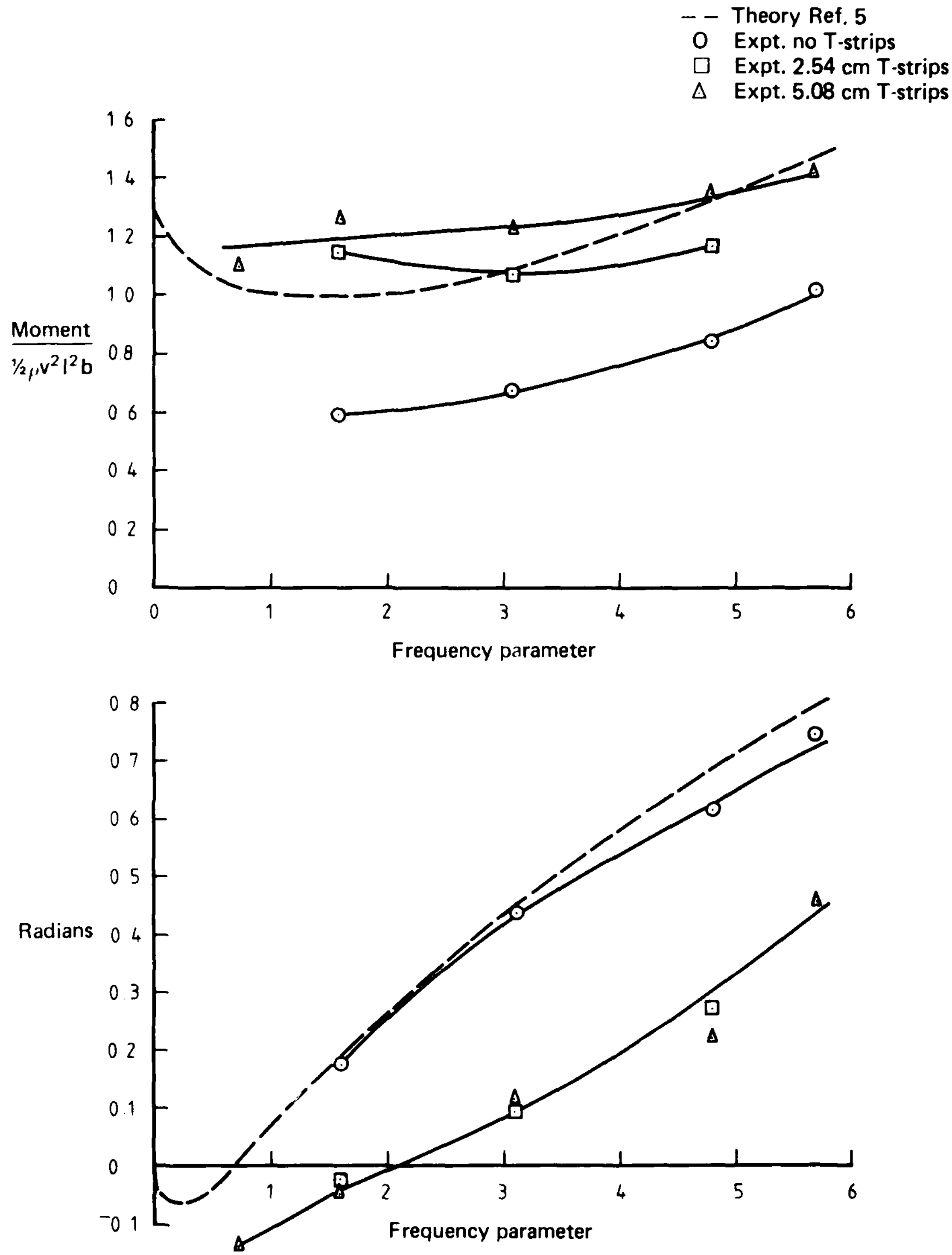

FIG. 16: COMPARISON OF THEORETICAL AND EXPERIMENTAL DERIVATIVES
(Moment about leading edge due to control rotation)

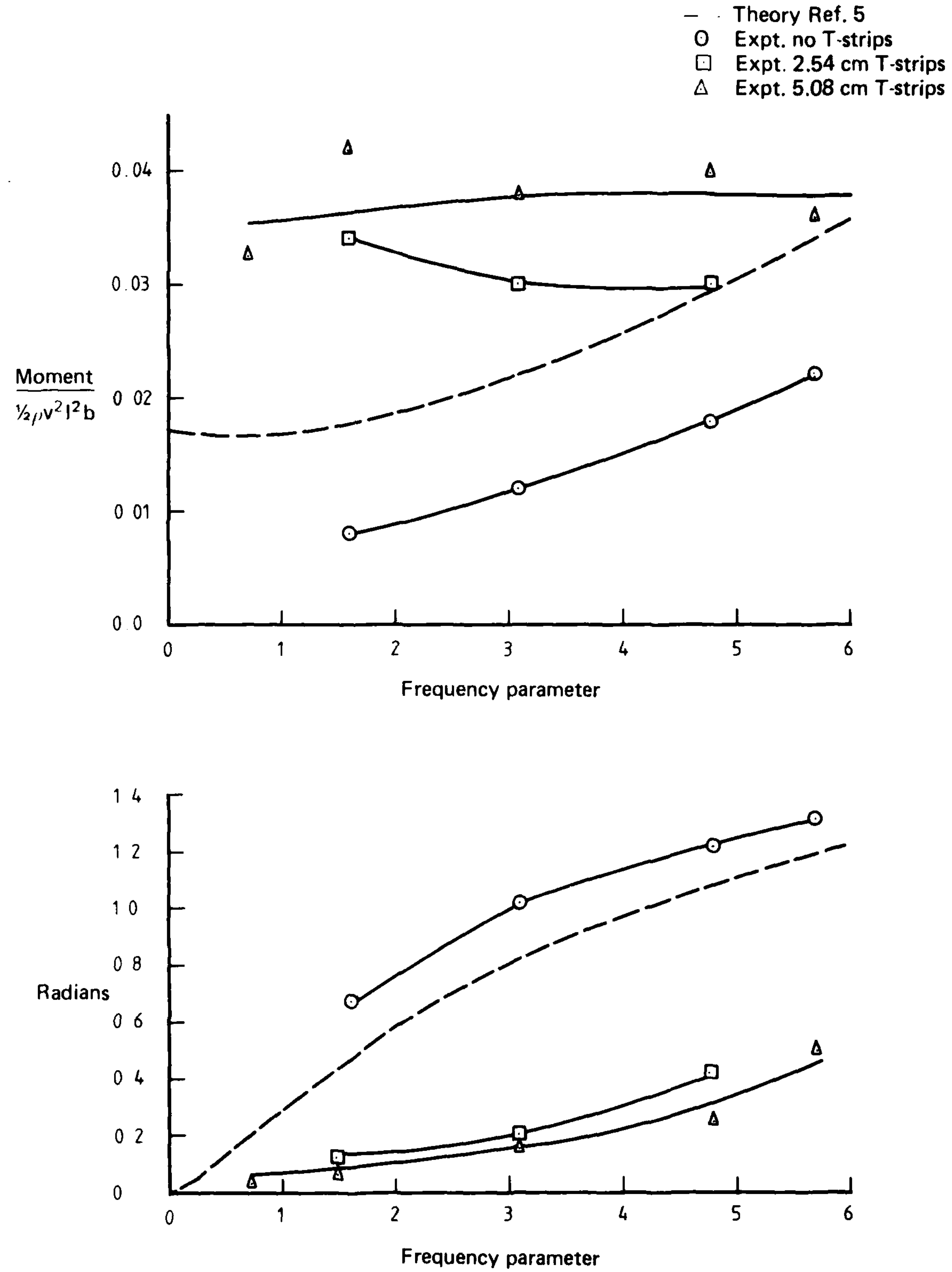

FIG. 17: COMPARISON OF THEORETICAL AND EXPERIMENTAL DERIVATIVES
(Hinge moment due to control rotation)

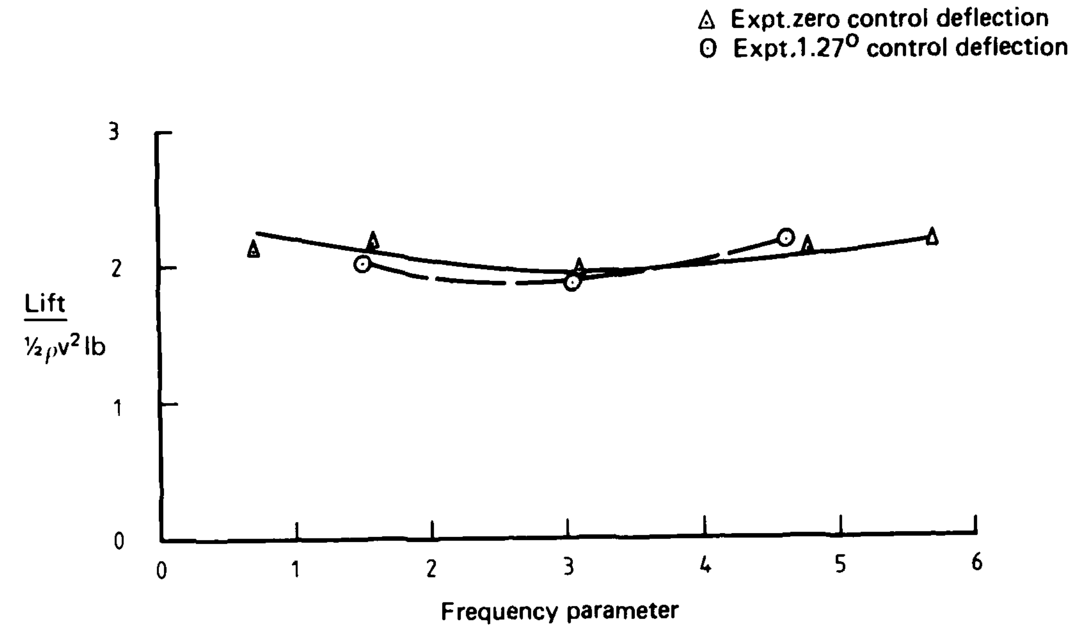

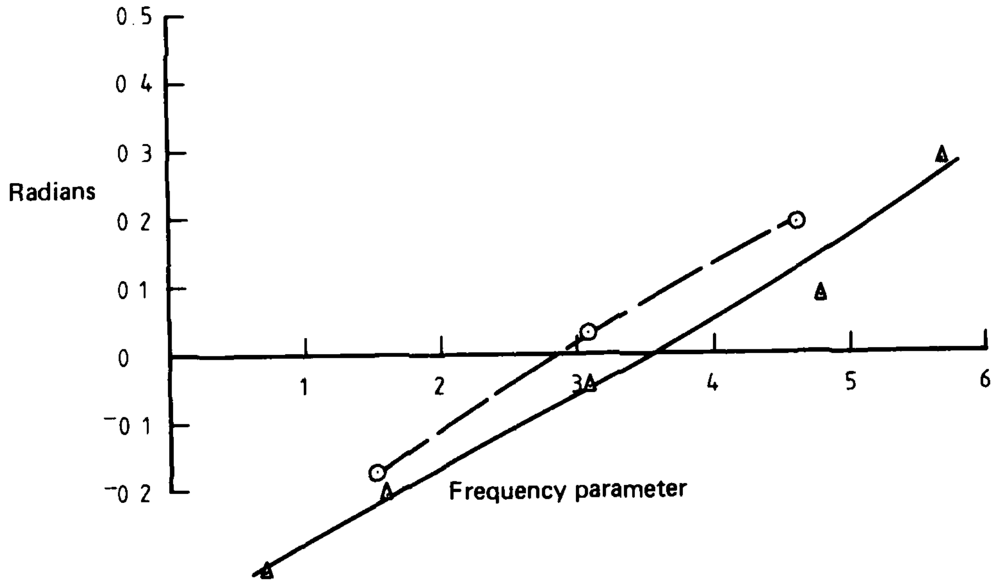

FIG. 18: EFFECT OF MEAN CONTROL DEFLECTION ON LIFT DUE TO CONTROL ROTATION (5.08CM T-STRIPS)

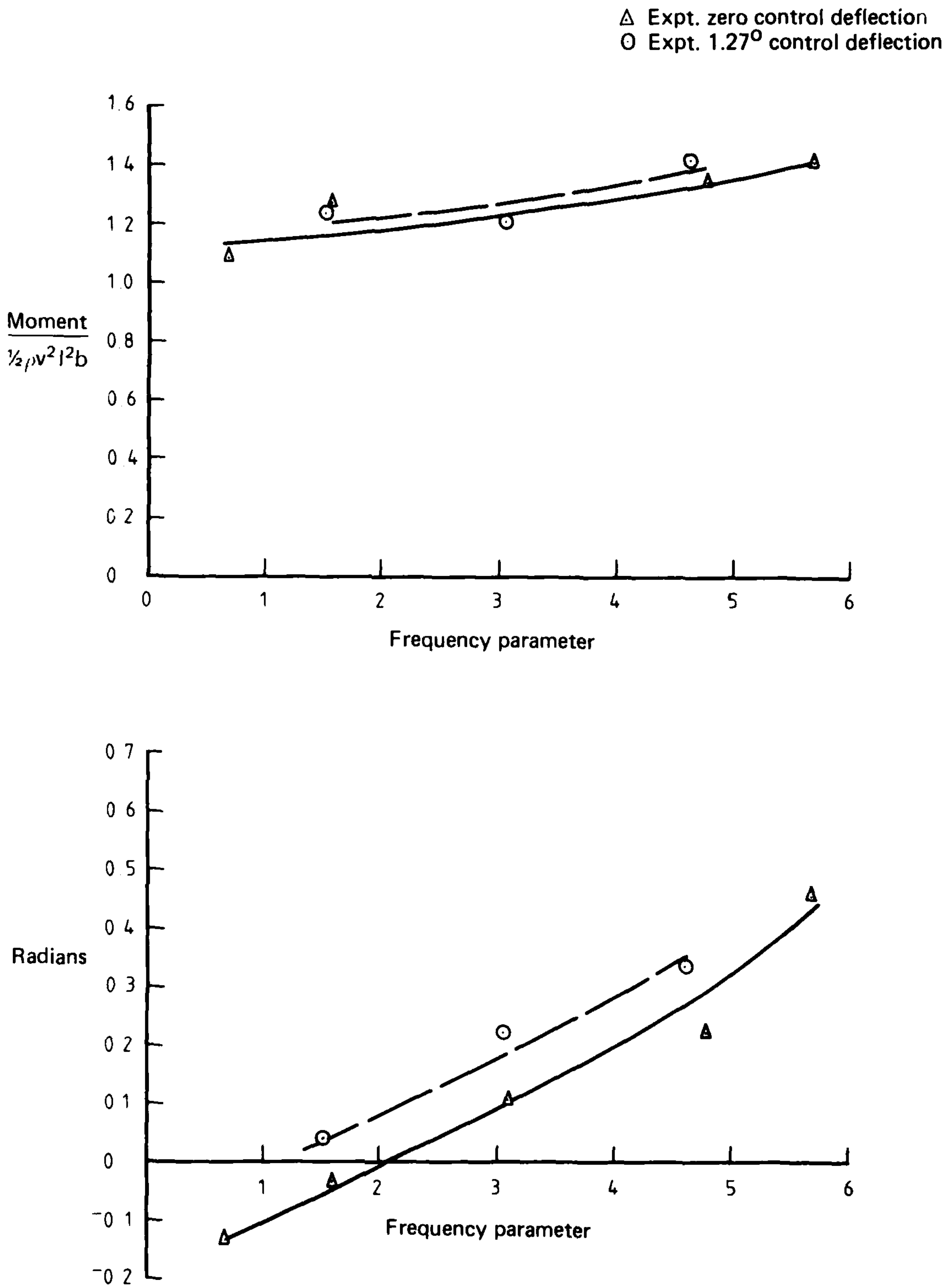

FIG. 19: EFFECT OF MEAN CONTROL DEFLECTION ON MOMENT ABOUT LEADING EDGE DUE TO CONTROL ROTATION (5.08CM T-STRIPS)

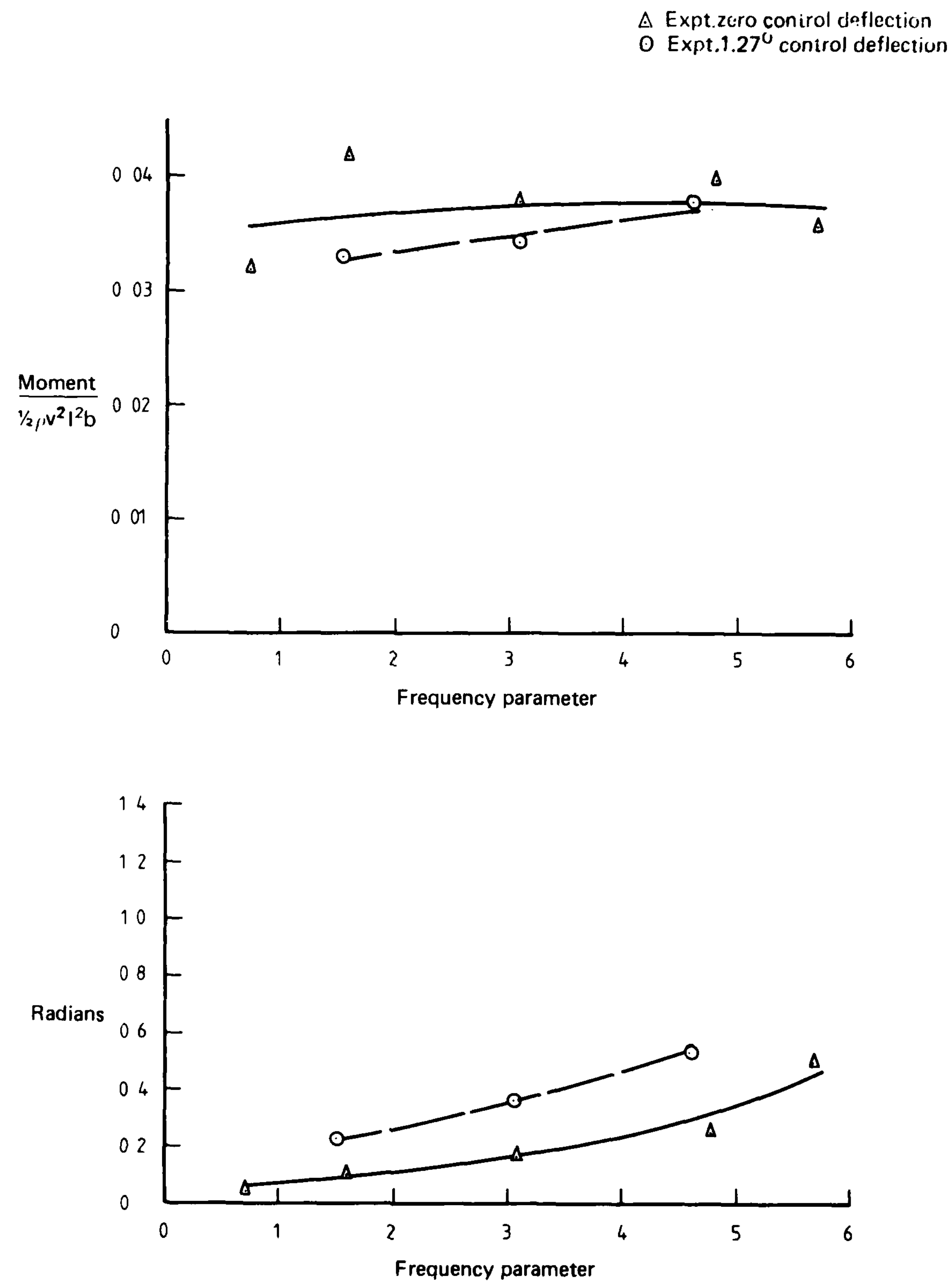

FIG. 20: EFFECT OF MEAN CONTROL DEFLECTION ON HINGE MOMENT DUE TO CONTROL ROTATION (5.08CM T-STRIPS)

DISTRIBUTION

	Copy No.
AUSTRALIA	
Department of Defence	
Central Office	
Chief Defence Scientist	1
Deputy Chief Defence Scientist	2
Superintendent, Science and Technology Programs	3
Australian Defence Scientific and Technical Representative (U.K.)	—
Counsellor, Defence Science	—
Joint Intelligence Organisation	4
Defence Library	5
Document Exchange Centre, D.I.S.B.	6–22
Aeronautical Research Laboratories	
Chief Superintendent	23
Library	24
Superintendent Structures Division	25
Divisional File — Structures	26
Authors: G. Long	27
P. A. Farrell	28
Superintendent Aerodynamics Division	29
T. Trimble	30
D. A. Lemaire	31
Materials Research Laboratories	
Library	32
Defence Research Centre, Salisbury	
Library	33
Defence Regional Office	
Library	34
Army Office	
Army Scientific Adviser	35
Royal Military College Library	36
Air Force Office	
Aircraft Research and Development Unit, Scientific Flight Group	37
Air Force Scientific Adviser	38
Technical Division Library	39
D.Air Eng.-AF	40
HQ Support Command (SENGSO)	41
RAAF Academy, Point Cook	42
Department of Productivity	
Government Aircraft Factories	
Manager	43
Library	44
Mr P. Hughes	45
Mr P. Scott	46

Department of Transport

Secretary		47
Library		48
Airworthiness Group, Mr K. O'Brien		49
Mr M. G. Chandivert, AWES		50

Statutory, State Authorities and Industry

Qantas, Library		51
Trans Australia Airlines, Library		52
Ansett Airlines of Australia, Library		53
Commonwealth Aircraft Corporation:		
Manager		54
Manager of Engineering		55
Hawker de Havilland Pty. Ltd.:		
Librarian, Bankstown		56
Manager, Lidcombe		57

Universities and Colleges

Adelaide	Barr Smith Library	58
	Professor of Mechanical Engineering	59
Melbourne	Engineering Library	60
Monash	Library	61
Sydney	Engineering Library	62
Queensland	Library	63
Tasmania	Engineering Library	64
West. Australian	Library	65
R.M.I.T.	Library	66
	Mr H. Millicer	67

CANADA

CAARC Coordinator Structures		68
NRC National Aeronautical Establishment, Library		69

Universities and Colleges

McGill	Library	70
Toronto	Institute for Aerospace Studies	71

FRANCE

AGARD, Library		72
ONERA, Library		73
Service de Documentation, Technique de l'Aeronautique		74

GERMANY

ZLDI		75

INDIA

CAARC Co-ordinator Structures		76
Civil Aviation Department, Director		77
Defence Ministry, Aero Development Establishment, Library		78
Hindustan Aeronautics Ltd., Library		79
Indian Institute of Science, Library		80
Indian Institute of Technology, Library		81
National Aeronautical Laboratory, Director		82

ISRAEL

Technion - Israel Institute of Technology, Professor J. Singer		83

ITALY

Associazione Italiana di Aeronautica e Astronautica	84
Fiat Co., Dr G. Gabrielli	85

JAPAN

National Aerospace Laboratory, Library	86

Universities

Tohoku (Sendai)	Library	87
Tokyo	Inst. of Space and Aeroscience	88

NETHERLANDS

Central Org. for Applied Science Research TNO, Library	89
National Aerospace Laboratory (NLR) Library	90

NEW ZEALAND

Librarian, Defence Scientific Establishment	91
Transport Ministry, Civil Aviation Division, Library	92
Transport Ministry, Mr J. Barclay	93

Universities

Canterbury	Library	94

SWEDEN

Aeronautical Research Institute	95
Research Institute of the Swedish National Defence	96

SWITZERLAND

Institute of Aerodynamics, Professor J. Ackeret	97

UNITED KINGDOM

Aeronautical Research Council, Secretary	98
CAARC, Secretary	99
Royal Aircraft Establishment:	
Farnborough, Library	100
Bedord, Library	101
National Physical Laboratories, Library	102
British Library, Science Reference Library	103
CAARC Co-ordinator, Structures	104
Aircraft Research Association, Library	105
Rolls-Royce (1971) Ltd., Aeronautics Division, Chief Librarian	106
British Aerospace Corporation:	
Aircraft Group, Kingston-Brough Division	107
Aircraft Group, Manchester Division	108
Aircraft Group, Headquarters Lab. Kingston-Upon-Thames	109
Dynamics Group, Hatfield Lostock Division	110
Aircraft Group, Weybridge — Bristol Division	111
Aircraft Group, Warton Division	112
British Hovercraft Corporation Ltd., Library	113
Short Brothers Harland	114
Westland Helicopters Ltd.	115

Universities and Colleges

Bristol	Library, Engineering Dept.	116
Cambridge	Library, Engineering Dept.	117
Liverpool	Fluid Mechanics Division	118
London	Professor A. D. Young, Aero Eng.	119
Belfast	Dr A. Q. Chapleo, Dept. of Aero. Engineering	120

Manchester	Professor N. Johannessen, Fluid Mechanics	121
Nottingham	Library	122
Southampton	Library	123
Strathclyde	Library	124
Cranfield Institute of Technology	Library	125
Imperial College	The Head	126

UNITED STATES OF AMERICA

NASA Scientific and Technical Information Facility	127
American Institute of Aeronautics and Astronautics	128
Applied Mechanics Review	129
The Chemical Abstracts Service	130
Bell Helicopter Textron	131
Boeing Co.:	
Head Office, Mr R. Watson	132
Industrial Production Division	133
Cessna Aircraft Co., Executive Engineer	134
Lockheed California Company	135
Lockheed Georgia Company	136
McDonnell Douglas Corporation, Director	137
United Technologies Corporation, Fluid Dynamics Laboratories	138
Battelle Memorial Institute, Library	139

Universities and Colleges

Florida	Aero. Engineering Dept.	140
Stanford	Dept. of Aero., Library	141
Polytechnic Institute of New York	Aeronautical Labs., Library	142
California Institute of Technology	Graduate Aero. Labs., Library	143
Massachusetts Institute of Technology	Library	144

Spares 145-154

MED

8